

# Advancements of $^{52g}\text{Mn}$ Production for Multi-Modal Imaging: Comparison of Production Routes with Natural Chromium and Vanadium Targets

F. Barbaro<sup>1,2</sup>, L. De Nardo<sup>1,3</sup>, L. Meléndez-Alafort<sup>4,5</sup>, L. Canton<sup>1</sup>, M.P. Carante<sup>6</sup>, A. Colombi<sup>2,6</sup>, A. Fontana<sup>6</sup>

<sup>1</sup> INFN, Sezione di Padova, Padova, Italy. <sup>2</sup> Dipartimento di Fisica dell'Università di Pavia, Pavia, Italy.

<sup>3</sup> Dipartimento di Fisica dell'Università di Padova, Padova, Italy. <sup>4</sup> Istituto Oncologico Veneto IOV IRCCS, Padova, Italy.

<sup>5</sup> INFN, Laboratori Nazionali di Legnaro, Legnaro (Padova), Italy. <sup>6</sup> INFN, Sezione di Pavia, Pavia, Italy.

## INTRODUCTION

The radionuclide  $^{52g}\text{Mn}$  is of significant medical interest for the innovative PET-MRI multi-modal imaging technique. The most studied production route is based upon the nuclear reaction  $^{nat}\text{Cr}(p,x)^{52g}\text{Mn}$ , however recently also the alternative reaction  $^{nat}\text{V}(\alpha,x)^{52g}\text{Mn}$  has been taken into consideration [1], within the CSN5-METRICS project. The study revealed that the experimental data sets for that reaction are still very scattered and need to be improved, and that the standard simulations with nuclear reaction codes, such as TALYS, FLUKA and EMPIRE, are not fully adequate to describe the  $^{nat}\text{V}(\alpha,x)^{52g}\text{Mn}$  cross-section.

Recently, the cross-section  $^{nat}\text{Cr}(p,x)^{52g}\text{Mn}$ , and co-produced contaminants  $^{54}\text{Mn}$  and  $^{51}\text{Cr}$ , were measured in view to optimize the routine production of  $^{52g}\text{Mn}$  [2]. Those data turned out in agreement with previously published data and have improved the available nuclear data sets for each radionuclide. In the case of  $^{nat}\text{Cr}$  target, standard simulations with TALYS described the cross-section in agreement with the body of measured data.

In view of possible applications of Manganese radionuclides in medical imaging, it is important to assess the impact of the produced radionuclide and main contaminants in terms of dose released to the patient's organs. In [3], the effective dose burden, due to the use of  $^{52g}\text{Mn}$  as brain tracer under the simple  $\text{MnCl}_2$  chemical compound, has been analyzed with computational dosimetry codes. It was found that the radiation dose released by  $^{52g}\text{Mn}$  may be quite significant, due to its relatively long physical half-life and the emission of high-energy  $\gamma$  rays.

## RESULTS

In this study, to compare the production routes, we have sought to improve the theoretical  $^{nat}\text{V}(\alpha,x)^{52g}\text{Mn}$  cross section by a suitable tuning of the parameters of the TALYS code, since the Best Theoretical Evaluation (BTE) introduced in [1] appears not completely satisfactory (see dashed dotted line figure 1. We have adjusted the parameters governing the  $^{52}\text{Mn}$  level density in order to obtain a better agreement with the data, at least in the range below 40 MeV. These parameters modulate the theoretical level density obtained with Hartree-Fock-Bogoliubov approach according to the transformation:  $\rho(E) = \exp(c\sqrt{E-p})\rho_{HFB}(E-p)$ ,

where the parameters  $c$  and  $p$  produce a normalization and energy shift, respectively. In particular, we have considered the TALYS level-density keyword *ldmodel 6* and have adjusted with  $c = 0.4$  and  $p = -1.0$  the parameters for  $^{52}\text{Mn}$ , to improve that cross section (figure 1, red line). With the same parameter set, also the cross section for the main contaminant,  $^{54}\text{Mn}$ , is well reproduced, as seen in figure 2.

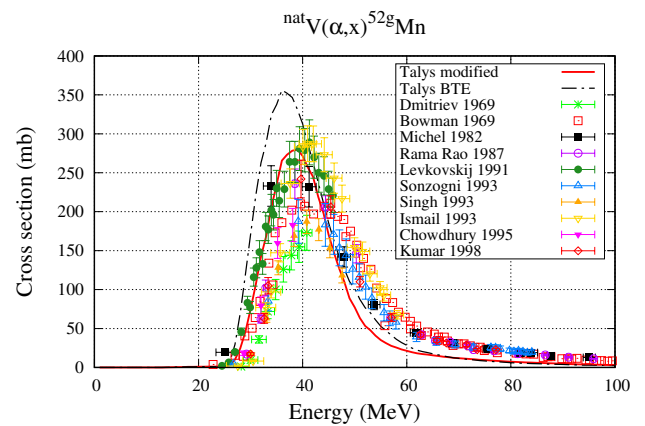


Fig. 1. Calculated cross section for  $^{nat}\text{V}(\alpha,x)^{52g}\text{Mn}$  (see text for explanation) and comparison with the collection experimental data available in EXFOR database.

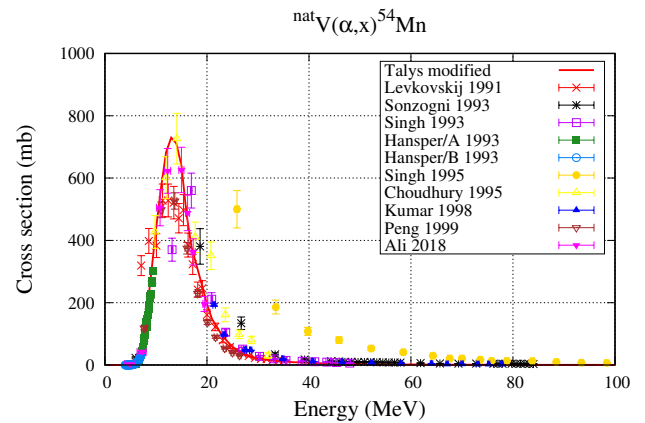


Fig. 2. Theoretical and experimental  $^{nat}\text{V}(\alpha,x)^{54}\text{Mn}$  cross section.

The reaction  $^{nat}\text{Cr}(p,x)^{52g}\text{Mn}$  was well reproduced with standard TALYS calculations and we report in figure 3 the results discussed in [1], without further adjustments.

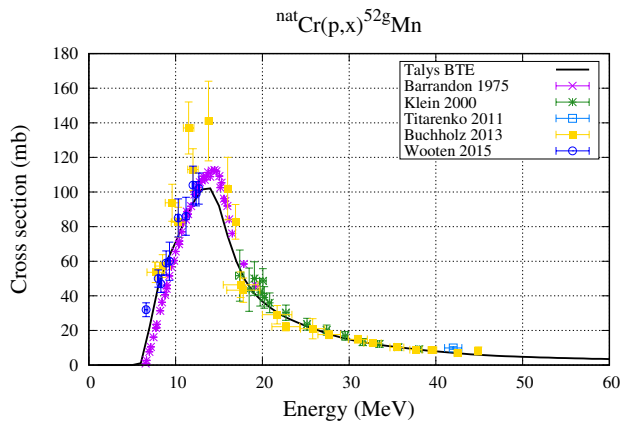


Fig. 3. Theoretical and experimental  $^{nat}\text{Cr}(p,x)^{52g}\text{Mn}$  cross section.

The expected yields for the radionuclide of interest and correlated impurities have been evaluated with irradiation conditions of  $1\ \mu\text{A}$  (beam current), 1 h (irradiation time), and  $200\ \mu\text{m}$  (target thickness). They are reported in table 1, where we have also included the estimation of the theoretical-model variance derived in [1].

Table 1. Predicted activity for  $^{52g}\text{Mn}$  and main contaminant  $^{54}\text{Mn}$  for both  $^{nat}\text{Cr}$  and  $^{nat}\text{V}$  target. The energy range  $[E_i-E_o]$  corresponds to a  $200\ \mu\text{m}$  target thickness, where  $E_i$  and  $E_o$  are the energy of the projectile impinging on the target and leaving the target, respectively.

Reaction $[E_i-E_o]$ (MeV)	Talys yield
$^{nat}\text{V}(\alpha,x)^{52g}\text{Mn}$ [48-33.9]	$5.16 \pm 1.04\ \text{MBq}/\mu\text{Ah}$
$^{nat}\text{Cr}(p,x)^{52g}\text{Mn}$ [17-14]	$4.40 \pm 0.51\ \text{MBq}/\mu\text{Ah}$
$^{nat}\text{V}(\alpha,x)^{54}\text{Mn}$ [48-33.9]	$2.71 \pm 0.22\ \text{kBq}/\mu\text{Ah}$
$^{nat}\text{Cr}(p,x)^{54}\text{Mn}$ [17-14]	$4.89 \pm 0.07\ \text{kBq}/\mu\text{Ah}$

The time-evolution of the produced activities, including those of the contaminants, have been determined and will serve as starting point for the subsequent dose-release assessments. From these quantities, the radionuclidic purity has been calculated comparing the outcomes between the  $^{nat}\text{Cr}$  and  $^{nat}\text{V}$  routes, as shown in figure 4.

## CONCLUSIONS

In this work, with the tuning of the parameters  $c$  and  $p$  governing the  $^{52}\text{Mn}$  level density, we have overcome a problem, found in [1], concerning the theoretical description of the  $^{nat}\text{V}(\alpha,x)^{52g}\text{Mn}$  reaction. We have evaluated the time evolution of the produced  $^{52g}\text{Mn}$  quantity, and its main impurities, as well as the corresponding activities. The production route with  $^{nat}\text{V}$  shows clear advantages in terms of radionuclidic purities, if compared with  $^{52g}\text{Mn}$  production

from  $^{nat}\text{Cr}$  targets.

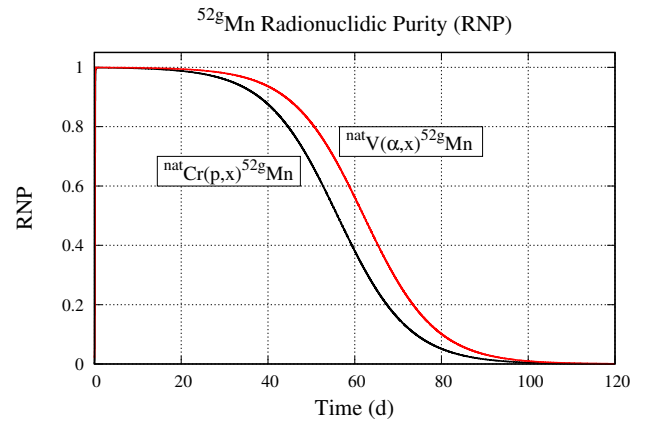


Fig. 4. Radionuclidic purity for the reactions  $^{nat}\text{Cr}(p,x)^{52g}\text{Mn}$  and  $^{nat}\text{V}(\alpha,x)^{52g}\text{Mn}$ , for  $1\ \mu\text{A}$  beam current and 1 h irradiation time.

## OUTLOOK ON DOSE-RELEASE ASSESSMENTS

To ensure the safety of a radiopharmaceutical for clinical application, the European Pharmacopoeia requires that radionuclides production methods generate a minimal amount of radioisotopic contaminants [4]. In general, the radionuclidic impurities limits are expressed as a percentage and from a pharmaceutical/GMP viewpoint should be set lower than 1%. However, to establish the minimal purity of new radiopharmaceuticals, not only the percent of radionuclidic impurities produced must be considered, but also the Dose Increase (DI) caused by these impurities. A good starting point to set the limits is to assure that the DI would be maintained within the 10% limit [5]. To check the fulfillment of this requirement, it is therefore fundamental to assess the absorbed dose due to all the radionuclides impurities co-produced with  $^{52g}\text{Mn}$ . This will be performed using the activities of  $^{52g}\text{Mn}$  and impurities calculated for both  $^{nat}\text{V}$  and  $^{nat}\text{Cr}$  targets, using the already assessed absorbed doses due to  $^{52g}\text{MnCl}_2$  and  $^{51}\text{MnCl}_2$  [3] and extending the calculations to other impurities. In this way it will be possible to identify the irradiation conditions with the best compromise between activity and purity and to determine the time window after the EOB in which this radioisotope could be used to label a radiopharmaceutical with an acceptable radionuclidic purity and DI to the patient.

- 
- [1] A. Colombi et al., arXiv, 2102.12228 (2021).
  - [2] R. El Sayed et al., Appl. Radiat. Isot., 147 (2019) 165.
  - [3] L. De Nardo et al., Appl. Radiat. Isot., 153 (2019) 108805.
  - [4] EANM 2019 *Radiopharmacy: An Update*. Published by European Association of Nuclear Medicine, available at: <https://www.eanm.org/publications/technologists-guide>
  - [5] L. De Nardo et al., Phys. Med. Biol., 66 (2021) 025003.